



Determination of denudation rates by the measurement of meteoric ^{10}Be in Guadiana river sediment samples (Spain) by low-energy AMS

S. Padilla^{a,b,*}, J.M. López-Gutiérrez^{a,c}, D.M.R. Sampath^d, T. Boski^d, J.M. Nieto^e, M. García-León^{a,f}

^a Centro Nacional de Aceleradores (Universidad de Sevilla, Consejo Superior de Investigaciones Científicas, Junta de Andalucía), Thomas Alva Edison 7, 41092 Seville, Spain

^b Laboratorio Nacional de Espectrometría de Masas con Acelerador (LEMA), Dpto. Física Nuclear y Aplicaciones de la Radiación, Instituto de Física, Universidad Nacional Autónoma de México (UNAM), Apartado Postal 20-364, 01000 Ciudad de México, Mexico

^c Dpto. de Física Aplicada I, Escuela Universitaria Politécnica, Universidad de Sevilla, Virgen de África 7, 41011 Seville, Spain

^d CIMAR, Centre for Marine and Environmental Research, University of Algarve, 8005-139 Faro, Portugal

^e Dpto. Geología, Facultad de Ciencias Experimentales, Universidad de Huelva, Av. 3 de Marzo, S/N, 21071 Huelva, Spain

^f Dpto. de Física Atómica Molecular y Nuclear, Universidad de Sevilla, Reina Mercedes s/n, 41012 Seville, Spain



ARTICLE INFO

Keywords:

^{10}Be
Deposition flux
Denudation rate
Guadiana river basin
SARA
Sediment budget method

ABSTRACT

The concentration of meteoric ^{10}Be in estuarine sediment samples has been measured by Spanish Accelerator for Radionuclides Analysis (SARA) at CNA and subsequently used to assess the denudation rate in Guadiana river basin together with the sediment budget method, on both sides of the frontier between Spain and Portugal. The two methods yielded coincident results. The estimation by the ^{10}Be method gave the denudation rate of $(0.76 \pm 0.10) \times 10^{-2} \text{ cm/y}$. After correcting for an approximate 80% attenuation of the sediment discharge into the ocean, caused by the river dams, the sediment budget method yielded the rate of $(0.77 \pm 0.17) \times 10^{-2} \text{ cm/y}$.

1. Introduction

Erosion and sedimentation responses to the changes occurring in hydrographical basins or in fluvial channels are of broad scientific and practical interest in agriculture, forestry and territorial management in general. There is a need to predict how the land use would affect the erosion and sedimentation as well as the relative importance of the different sediment sources to prioritize measures of erosion control. It is necessary to anticipate the location of sediment deposition, the storage duration and their re-mobilisation, therefore, a precise estimation of denudation rate can be used to estimate the temporal variability of the sediment retention rate within the upstream of the estuary limits.

In the recent years, great progress in several areas was achieved thanks to the application of meteoric ^{10}Be in terms of the measurements of soil profile ages, denudation rates, production models in the atmosphere, the influence of the weather on its production or solar activity (Field et al., 2006; Heikkilä, 2007). ^{10}Be is a radionuclide which may be found in water, soil and rocks in very low concentration such as 10^7 atm/g in sediments, 10^7 atm/m^3 in aerosol filters, 10^5 atm/L in rain waters or 10^4 atm/g in ice cores (von Blanckenburg, 2005; von Blanckenburg et al., 1996). It is produced by interaction of cosmic rays

with atmospheric ^{16}O and ^{14}N (meteoric) and ^{16}O within mineral lattices at the Earth's surface (in situ) through spallation reactions (Fig. 1a). Meteoric ^{10}Be is primarily produced in the lower Stratosphere and upper Troposphere. The average residence time in the atmosphere ranges between two weeks and several years, depending on the origin layer (Troposphere or Stratosphere). The production, Stratosphere-Troposphere exchanges, as well as transport and tropospheric deposition, modulate the fluxes to the Earth surface, and influence the ^{10}Be concentrations at the surface (Graly et al., 2010). ^{10}Be attached to aerosols particles in the atmosphere is carried to the lower Troposphere and deposited at the Earth surface, either by rain, in soluble form or by dry deposition (Field et al., 2005). Once on the surface, the high reactivity of hydrolyzed ^{10}Be at most natural pH levels ensures that meteoric ^{10}Be is readily adsorbed to particles in the upper meters of soil profiles (von Blanckenburg et al., 2012), serving as a tracer of the path taken by soil particles. Sedimentary systems can record the long-term deposition of meteoric ^{10}Be even after complex pathways due to the chemical leaching, dissolution by rain, erosion or mixing in soils. Hence meteoric ^{10}Be has a great potential to be used as a geochemical tracer for denudation rate (Ebert et al., 2012; Masarik and Beer, 1999).

The denudation rate in a drainage basin is also very useful for the

* Corresponding author. Laboratorio Nacional de Espectrometría de Masas con Acelerador (LEMA), Dpto. Física Nuclear y Aplicaciones de la Radiación, Instituto de Física, Universidad Nacional Autónoma de México (UNAM), Apartado Postal 20-364, 01000 Ciudad de México, Mexico. Tel.: +5556225159; fax: +55 56225009.

E-mail address: spadilla@fisica.unam.mx (S. Padilla).

<https://doi.org/10.1016/j.jenvrad.2018.04.016>

Received 23 January 2018; Received in revised form 13 April 2018; Accepted 17 April 2018

Available online 26 April 2018

0265-931X/ © 2018 Elsevier Ltd. All rights reserved.

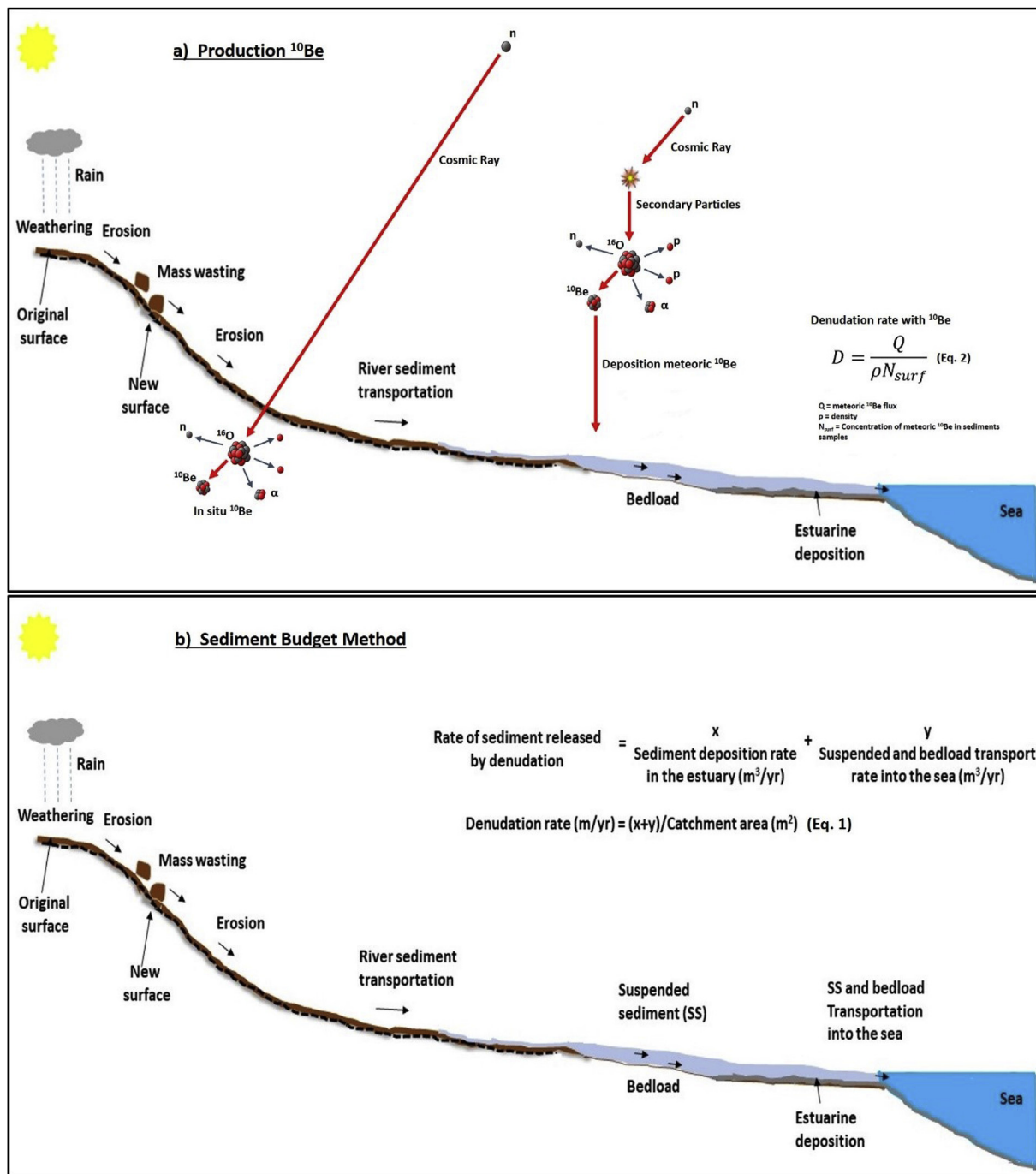


Fig. 1. a) Diagram of the production of both meteoric ^{10}Be in atmosphere and in situ ^{10}Be at the Earth's surface. The assessment of the denudation rate is calculated with the variables in Eq (2). b) Schematic diagram of a soil profile and definitions of variables for the assessment of the denudation rate by sediment budget method by Eq. (1).

study of the sediment filling models of estuarine systems. It refers to the total mass of solids removed from the shallow depth at Earth surface. It is the result of the combined effect of the physical (erosion) and chemical (weathering) processes. Since cosmogenic radionuclides collected into the material are continuously transferred to the ground surface, the total denudation rate (cm/y) can be measured. The estimations of the rate of the cosmogenic radionuclide transfer into soils reflect the denudation rate of fluvial geographical accidents, which are subject to geological processes such as weathering, mass movements and surface and fluvial flux. Those geological processes can be measured in time scales ranging from 10^3 to 10^7 years (von Blanckenburg, 2005; Willenbring and von Blanckenburg, 2010). The advantages of the

meteoric ^{10}Be over the insitu-produced nuclides consists in the higher concentrations of the former, requiring smaller sample amounts, its applicability to quartz-free lithologies, and the possibility to determine denudation rate time series in fine-grained fluvial or estuarine sediments. The interference of ^{10}Be produced in situ in these depositional settings may be easily eliminated by chemical stripping from the grain surface (meteoric) and dissolution of the mineral (in situ produced) (Willenbring and von Blanckenburg, 2010).

The sediment budget method for a river catchment has to take into account all the sources and deposition of the sediment as well as its transportation from the origin to its evacuation from a drainage basin, usually called the yield (Wasson, 2003). In its complete form, the

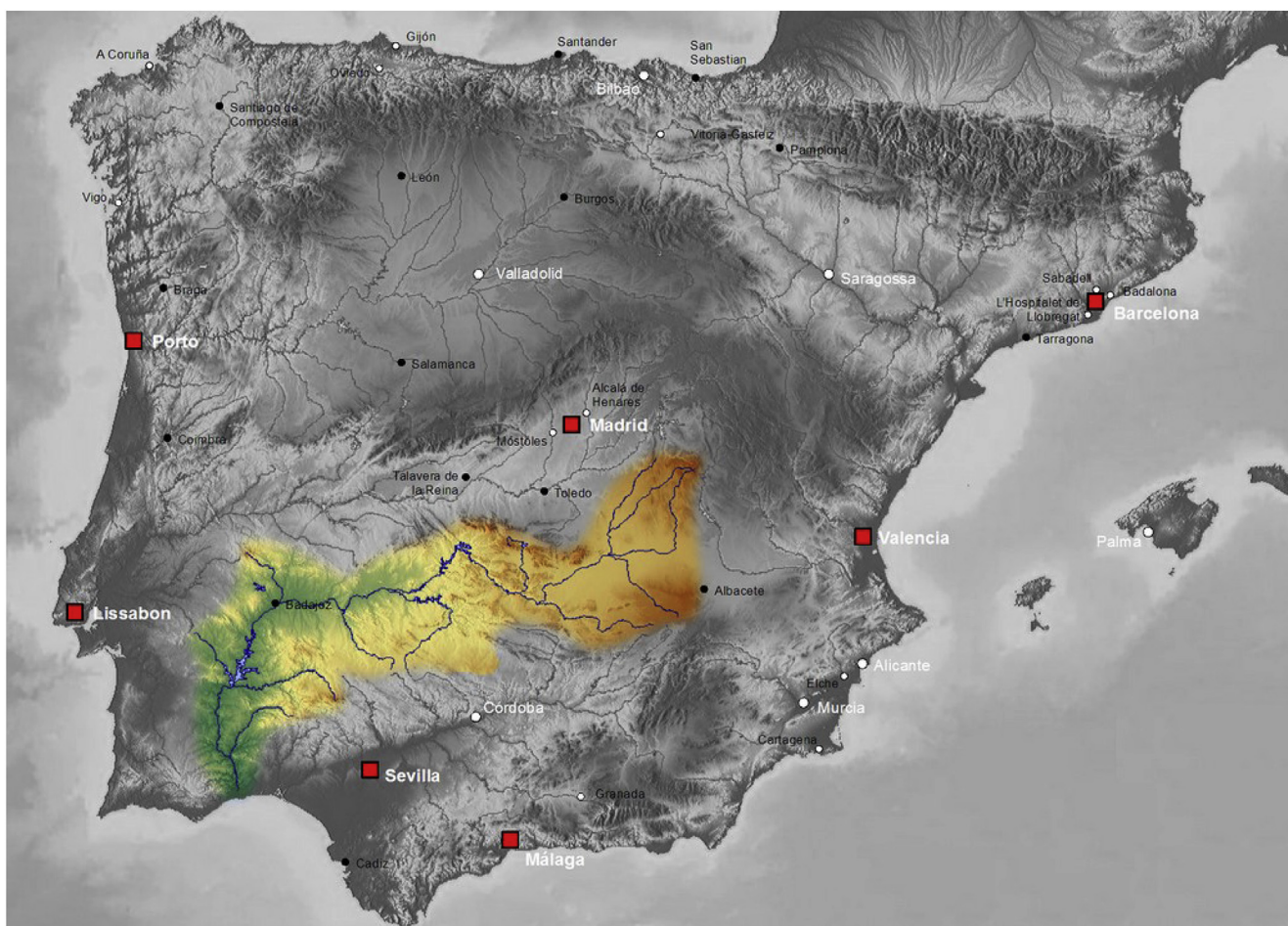


Fig. 2. Guadiana river hydrographical or drainage basin (<http://www.chguadiana.es/>).

sediment budget method represents the rate of erosion combined with the transportation of the sediment through the fluvial channels, its temporary storage in bars, banks and alluvial fans, as well as its weathering and breakdown during transport and storage (Reid and Dunne, 2000). Usually, the sediment budget also includes measurements of the residence time of the sediment in the intermittent traps, thus providing the data necessary for estimating the long-term impacts. Then, the results can be combined to produce an estimation of the sediment fluxes in several transport paths within the drainage the basin (Fig. 1b). The data can be used to assess the magnitude of the changes in the production of the sediment and the relative importance of sediment sources (Reid et al., 1981). The denudation rate in the drainage basin and the subsequent transfer to the ocean-continent interface is a key parameter for forecasting the evolution of coastal systems like estuaries, deltas and lagoons. This is of particular importance for the estuarine/deltaic areas like the Guadiana Estuary because of the accelerating sea-level rise on one hand and the retention of land born sediments behind the river dams on the other.

In order to assess the coherence of the information based on ^{10}Be data we confronted denudation rate derived from the ^{10}Be measurement with the result obtained by the sediment budget method. The study was applied to the samples from the estuary of Guadiana River making the border between Spain and Portugal in the SW Iberian Peninsula.

2. Geographical and hydrodynamic setting

The Guadiana River has its sources in Lagunas de Ruidera in Spain, at 1700 m altitude, and runs 810 km until reaching the Atlantic Ocean, between the Portuguese town Vila Real de Santo António and the

Spanish town Ayamonte. Located between 37° and 40° N and between 2° and 8° W, its catchment area covers $66\,889\text{ km}^2$ (Fig. 2). The estuary is funnel-shaped, deeply incised terminal part of river valley, infilled with post-glacial sediments (Boski et al., 2008). Currently, it is in advanced state of sediment infilling, with the formation of a flood delta in its mouth caused by the interaction of coastal sedimentation processes and a relatively stable sea level. According to the chemical definition of an estuary it is located along a 10 km of the terminal of boundary between Portugal and Spain, in a semi-arid region with a Mediterranean climate (Martinez-Aldaya and Llamas, 2009), characterized by a pronounced inter-annual variability, with sporadic rainy years alternating with years of droughts (Boski et al., 2008). As a result, river inputs to Guadiana estuary are highly variable resulting, at a seasonal and inter-annual scale, in droughts and episodic floods in the river basin. In the period 1947–2001, the monthly river discharge ranged from $< 10\text{ m}^3/\text{s}$ to $4660\text{ m}^3/\text{s}$ and 50% of the recorded values were less than $110\text{ m}^3/\text{s}$ (Fortunato and Oliveira, 2004). The mean river flow measured at Pulo do Lobo station (about 85 km upstream from river mouth) during summer reached $20\text{--}25\text{ m}^3/\text{s}$ during 1997 and 1998, before the closure of Alqueva dam and decreased below $10\text{ m}^3/\text{s}$ from 1999 to 2003, during the Alqueva dam construction and filling (Galvão et al., 2012). The estuary exhibits a semi-diurnal, meso-tidal regime with a mean range of approximately 2.5 m. The mean neap tidal range is 1.22 m and the mean spring tidal range is 2.82 m with a maximum spring tidal range of 3.5 m (Garel et al., 2009). In the context of rapid sea-level rise in the 21st century, the reduction of fluvial sediment supply due to the regulation of river discharge represents a major challenge for the management of estuarine ecosystems such as salt marshes and the reduction of sediment into the sea also result in severe erosion of the

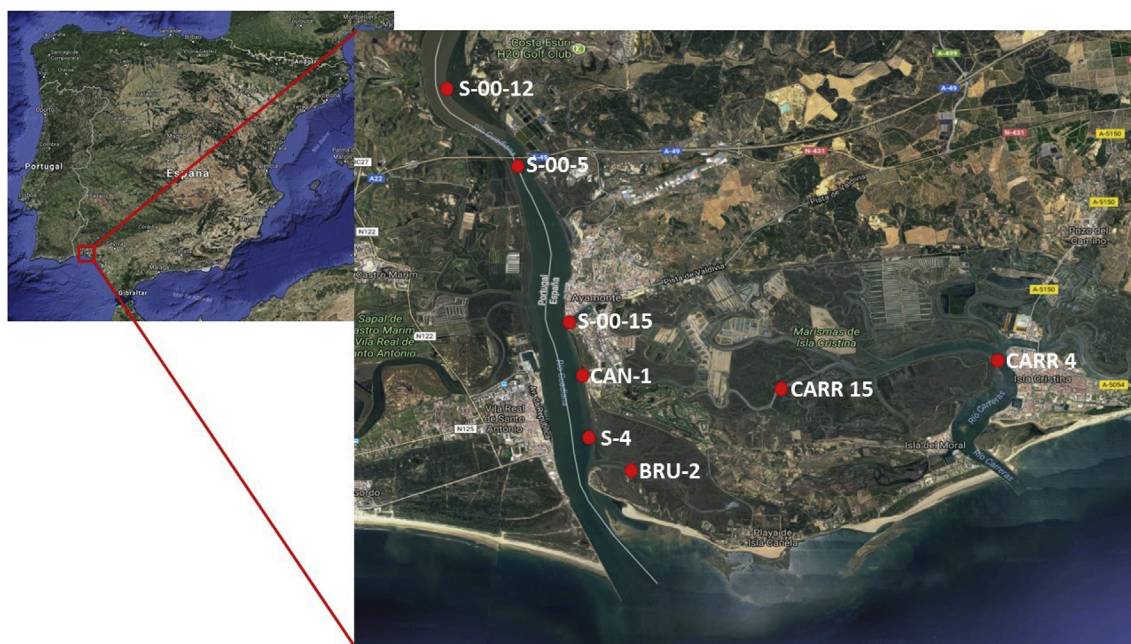


Fig. 3. Sampling zone within the Guadiana river catchment (Delgado et al., 2011).

Guadiana coastal systems including its eastern shoreface (Sampath and Boski, 2016). Therefore, a precise estimation of denudation rate can be used to estimate the temporal variability of the sediment retention rate within the upstream of the estuary limits, which is about 60 km above the river mouth. Thereby, a coastal zone management strategy can be developed to adapt to the impacts on the lower Guadiana estuary habitats and shoreface erosion due to flow regulations in the upstream of the estuary.

3. Sampling and sample preparation

For sampling of surficial sediments, 8 representative sampling points in the estuarine area were selected, in 2008. The sampling points were located in the lower estuary within 10 km of the shoreline, representing almost entire mixing zone of the estuary (Fig. 3). The surface sediments correspond to the intertidal flats along principal channels in the estuary. They included the main channel of the Guadiana River itself and the stream channels in the Spanish basin such as “La Canela”, “San Bruno” and “Carreras”. The channels sites were chosen to represent active sediment deposition environment. (Delgado et al., 2011). The sample profiles are shown in Table 2. The purpose of the sample

Table 1

Meteoric ^{10}Be deposition flux values reported by U. Heikkilä (Q in equation (2)), obtained by simulation by ECHAM5-HAM for every month along 2008 on Guadiana river [22].

Month 2008	Deposition flux meteoric ^{10}Be (Q) (10^9 atoms/ m^2/y)
January	5.85
February	10.32
March	14.32
April	11.47
May	19.49
June	9.07
July	1.35
August	0.33
September	0.79
October	7.96
November	3.47
December	13.28
Average value	8.14 ± 1.74

preparation procedure was to extract Be from sediments and convert it to BeO , which can then be used as target for the AMS measurement. The procedure of leaching and extraction of Be from river sediment samples (Fig. 4) has been adapted to our laboratory from (Gutjahr et al., 2007; Lachner et al., 2013).

About 1 g aliquot was taken from the river sediment sample. The carbonate fraction contained in the sample was dissolved and a first leaching was carried out in 40 mL acetate buffer (pH 4.66) shaken for 2 h, then centrifuged (4000 r.p.m. 10 min) to finally remove the supernatant. The Be fraction was extracted from the solid in a second leaching in 40 mL of 0.05 M hydroxyl-amine hydrochloride in 15% acetic acid, and buffered to pH 4 with NaOH. After 2 h of shaking, Fe-Mn oxihydroxide was dissolved into the sample. After centrifugation, the supernatant was evaporated in a beaker with 250 μl of ^9Be carrier ($\text{Be}_4\text{O}(\text{C}_2\text{H}_3\text{O}_2)_6$ standard 1000 mg/l to ICP, Merck) and re-dissolved in about 8 mL 6 M HCl. The Fe was separated on a column containing 2 mL Bio-Rad AG1x8 (100–200 mesh) resin. The resin was first rinsed with 10 mL MilliQ water, cleaned with 10 mL 0.3 M HCl and conditioned with 6 mL 6 M HCl. The sample was then loaded onto the column and the fraction was collected immediately. The column was afterwards rinsed with 6 mL 6 M HCl. The solution (6 mL 6 M HCl) was then collected and combined with the Be fraction for further processing. The solution was then evaporated and re-dissolved in about 10 mL 0.4 M oxalic acid. The Ca into material may be precipitated at this stage. After centrifugation, the supernatant was again evaporated and re-dissolved in 10 mL oxalic acid. The next purification step was carried out on 2 mL columns of Bio-Rad AG50x8 (200–400 mesh). The resin was cleaned with 12 mL 5 M HNO_3 and rinsed with 16 mL MilliQ water. Afterwards, the resin was conditioned with 16 mL 0.4 M. The sample was then loaded onto the column and the sample was washed with 4 mL 0.4 M oxalic acid. Further cations like Fe, Al and Ti were removed with 24 mL 0.4 M oxalic acid. After rinsing with 8 mL MilliQ water, 12 mL 0.5 M HNO_3 was used to elute Na. Finally, the Be fraction was collected in 30 mL 1 M HNO_3 (Lachner et al., 2013). The dissolution of Be was evaporated and dissolved in 1 mL pure HNO_3 . The sample was then loaded onto a centrifuge tube and the beaker was cleaned with 10 mL of water. The Be was precipitated into $\text{Be}(\text{OH})_2$ with Ammonia (pH 9). After centrifugation, the supernatant was removed and the solid was calcined into BeO in an oven at 1000 °C in a crucible during 1 h. Afterwards it was mixed with about 4 mg Nb powder. Finally, the

Table 2

Characteristics, average values obtained for the ratios and for the ^{10}Be (atoms/g) concentrations in Guadiana river sediment samples and the assessment of the denudation rate (D) using equation (2).

Sample	Position		Mass (g)	$^{10}\text{Be}/^9\text{Be}$ (10^{-12})	^{10}Be (N_{surf}) (10^7 atoms/g)	Density (ρ) (kg/L)	Denudation rate (D) (10^{-2} cm/y) 2008	Average annual flux
	Latitude ($^{\circ}\text{N}$)	Longitude ($^{\circ}\text{W}$)						
CARR-4	37.20	-7.33	1.0028	2.48 ± 0.31	3.99 ± 0.11	2.679	0.76 ± 0.16	
CARR 15	37.19	-7.37	1.0033	3.32 ± 0.24	5.50 ± 0.12	2.684	0.55 ± 0.12	
CAN 1	37.20	-7.40	1.0037	3.29 ± 0.36	5.39 ± 0.12	2.683	0.56 ± 0.12	
BRU 2	37.18	-7.40	1.0022	2.75 ± 0.18	4.47 ± 0.11	2.684	0.68 ± 0.15	
S-4	37.18	-7.40	1.0007	1.74 ± 0.17	2.73 ± 0.10	2.680	1.11 ± 0.24	
S-00-5	37.23	-7.42	1.0008	2.56 ± 0.16	4.21 ± 0.11	2.678	0.72 ± 0.16	
S-00-12	37.24	-7.43	1.0031	2.07 ± 0.24	3.32 ± 0.10	2.677	0.92 ± 0.20	
S-00-15	37.21	-7.41	1.0065	1.59 ± 0.25	2.49 ± 0.10	2.673	1.22 ± 0.26	
						Average value	0.76 ± 0.10	

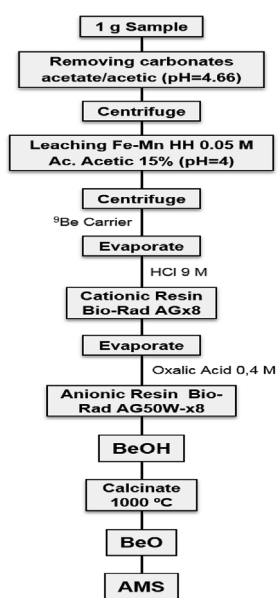


Fig. 4. Scheme for separation of the Al and the Be with ion exchange resins (Padilla Domínguez, 2015).

material was pressured into an Al cathode-holder and measured in SARA (Padilla Domínguez, 2015) (Fig. 4).

4. AMS measurement

The radionuclides were measured during 1 h each using the 1 MV AMS - Spanish Accelerator for Radionuclides Analysis - (SARA) system installed at the Centro Nacional de Aceleradores (CNA, Seville, Spain). SARA has a very compact design ($3.8 \times 6.3 \text{ m}^2$). On the low energy side, a Cs-Sputter SO110 ion source produces the negative ion beam within a vacuum about 1.4×10^{-7} mbar and a beam energy of 35 keV. It was mass-analysed by a 40 cm radius 90° sector magnet (low energy magnet), and accelerated in a 1 MV Tandem accelerator, stable in a voltage range from 0.1 to 1.1 MV, using argon gas in the terminal stripper. The beam was then analysed for mass and energy by a 85 cm radius 90° sector magnet (high energy magnet) and by a 120° electrostatic analyser (ESA). The ions were finally counted and identified in a two-anode gas ionization chamber provided with a 40 mm silicon nitride entrance window (Calvo et al., 2015). To separate the isobaric ^{10}B from ^{10}Be , a 75 nm thick silicon nitride foil is inserted in front of the electrostatic analyser in the path of the ^{10}Be . At the detector plane, the two beams are physically separated about 20 mm, and consequently the countrate in the detector from ^{10}B as well as the background is substantially reduced (Klein et al., 2006). The average currents obtained on the measurements of ^9Be isotopes in the high energy zone were around

1 μA . Measurements were carried out in charge state +1 for the Be after the accelerator and +2 after the passive absorber. The energy reached was 1403.61 keV for ^{10}Be . The ratios $^{10}\text{Be}/^9\text{Be}$ obtained were around $(1.59\text{--}3.32) \times 10^{-12}$ and the ^{10}Be concentrations were around $(2.49\text{--}5.50) \times 10^7$ atoms/g (Table 2). The results were normalized with Nishiizumi standard ^{10}Be -01-5-1 with a nominal $^{10}\text{Be}/^9\text{Be}$ ratio of 2.709×10^{-11} (Nishiizumi et al., 2007). The value for blank was $(5.39 \pm 1.34) \times 10^{-14}$ and the uncertainties of the results were found to be around 3% (Table 2).

5. Sediment budget method

Sediment budget method of estimating the denudation rate is essentially a mass balance based approach, which accounts the sources, sinks and redistribution pathways of sediments in a unit region over unit time (Slaymaker, 2003) and it is independent of ^{10}Be approach because the sediment budget approach depends on the direct processes involved with mass wasting. However, the ^{10}Be approach is a proxy to estimate the denudation rate of the catchment. According to Gregory and Goudie (2011), the simple form of the sediment mass balance relates the sediment inputs (I) from upstream, tributaries, and slopes to outputs (O) and a change in sediment storage (ΔS) due to deposition and erosion of the valley, floodplain and lacustrine sediment stores:

$$I = O \pm \Delta S \quad (1)$$

As the estimation of direct denudation measurements on slopes can lead to pitfalls, the denudation rate is usually derived from the determination of the sediment transport of streams or rivers (Ahnert, 1970). Accordingly, sediment load estimations or measurements give a value for the total mass of rock or soil removed from the drainage basin per unit time. If the average density of material is known, this mass can be converted into volume per unit time. If the basin area is known, then the thickness of removed material or the average denudation rate can be derived for the whole basin (Fig. 5).

Though there are no measured values for the suspended load and bedload sediment transport in the Guadiana estuary, estimation of these parameters by (Morales González, 1995; Portela, 2006) was used for the estimation of the denudation rate using the sediment budget method. The estimation of the annual rate of deposition of the sediment in the estuarine system, including the intertidal area was carried out by using the Hybrid Estuarine Sedimentation Model (Sampath et al., 2015). Using the HESM, the total fluvial sediment load deposited in the estuary, including the intertidal zone area of the lower Guadiana estuary is described below. The sea-level rise rate from 11500 Cal. y BP (Calendar years Before Present) to 7500 Cal. y BP was 7.5 mm/y and then up to the present pre-anthropogenic period, it was about 1.3 mm/y and it has kept pace with sea-level rise during the Holocene (Boski et al., 2008, 2002; Delgado et al., 2012).

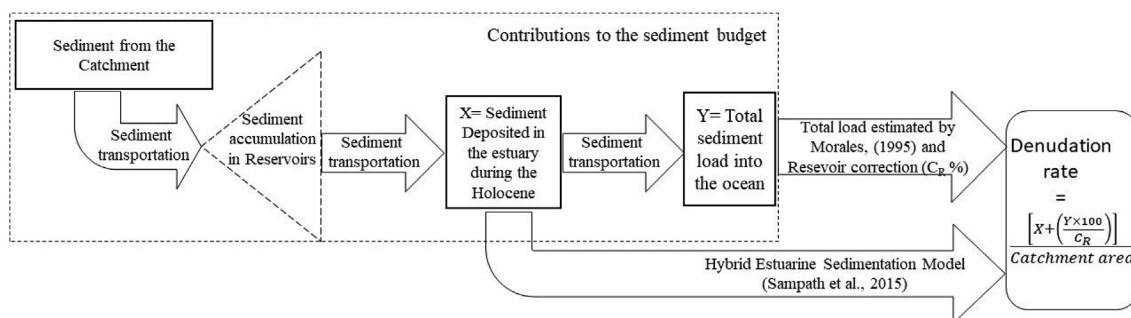


Fig. 5. Contributions to the sediment budget of the Guadiana River.

6. Results and discussion

6.1. Denudation rate based on Guadiana river samples

The assessment of denudation rate by the measurement of the concentration of the ¹⁰Be meteoric in Guadiana river sediment samples was reported by (Willenbring and von Blanckenburg, 2010). Those authors also reported an equation to calculate the denudation rate. The application to meteoric ¹⁰Be adsorbed within sediments follows the same approximation used for ¹⁰Be produced “in situ”, where the production of cosmogenic nuclides in a basin eventually equals the export of nuclides from the basin through erosion of sediment. This approximation is based on the equations used to calculate the inventory of ¹⁰Be, the concentration of ¹⁰Be at a certain depth (Eq. (2)) and the distribution of ¹⁰Be to the bottom of the soil. The concentration can be converted into a watershed steady state denudation rate. Taking into account the fact that the inventory of the watershed cannot be measured since it is a surficial sediment, an equation will be used to obtain denudation rate given the flux and the concentration of ¹⁰Be measured on the surface. The assumptions that are used to simplify this difficult problem as follow (Willenbring and von Blanckenburg, 2010).

1. The retention of ¹⁰Be is high, meaning that the nuclide is only lost as adsorbed on particles and not through solutions.
2. The flux of ¹⁰Be is known and is steady on long time scales.
3. The system is at steady state, meaning that the ¹⁰Be lost through erosion and decay from the system per unit time is equal to that entering by atmospheric flux.
4. The erosion rate remains approximately constant over a relevant time scale.

Finally, the following equation is used to make an approximation to calculate the denudation rate.

$$D = \frac{Q}{\rho N_{surf}} \tag{2}$$

where Q is the flux of ¹⁰Be into the surface (atom/m²·year), N_{surf} is the concentration of ¹⁰Be into the surface (atom/kg) and ρ is the density (kg/L). Equation (2) shows that the erosion rate is roughly proportional to the local flux divided by the surface concentration.

Using this equation, an estimation of denudation rate given as the mean annual value for all samples can be calculated using the mean annual value of the total flux through the whole year of 2008 (Tables 1 and 2). The flux deposition data of ¹⁰Be are reported by Ulla Heikkilä (Australia Natural Science and Technology Organisation, ANSTO, Australia) (personal communication). The data correspond with the meteoric ¹⁰Be flux (atom/m²·y) obtained by General Simulation Mode ECHAM5-HAM to ¹⁰Be. ECHAM5 is the fifth-generation atmospheric global circulation model (GCM) developed at the Max-Planck Institute for Meteorology, Hamburg. It solves the prognostic equations for vorticity, divergence, surface pressure and temperature, expressed in terms

of spherical harmonics with a triangular truncation. The additional aerosol module HAM includes the microphysical processes the emission and deposition (wet and dry) of aerosols, a sulfur chemistry scheme and aerosol impact radiation (Heikkilä et al., 2009). The model calculates its own precipitation and all other atmospheric parameters, so therefore there is no direct way to calculate any errors, other than to compare with observations (Ulla Heikkilä, personal communication). This simulation gives the mean monthly value for Guadiana river in 2008 at the coordinate 37°10'12" N and 7°23'37" W (Heikkilä and Smith, 2013), of the river mouth (Fig. 6). The variation of the values shown for each deposition flux indicate that the uncertainty obtained within the assessment of the average value in whole year 2008 is high (Table 1, Fig. 6), hence the denudation rate data have a high uncertainty also (Table 2, Fig. 7).

In order to calculate the denudation rate of the Lower Guadiana river basin we used the average deposition flux of ¹⁰Be in 2008 (Table 1), along with the sample density and the concentration of ¹⁰Be values obtained in our laboratory (Table 2). The denudation rates values obtained by applying equation (2) are shown in Table 2.

The estimation of denudation rates of Lower Guadiana river basin by measuring of meteoric ¹⁰Be in sediment samples using the average annual deposition flux were obtained. The average value for all sample measurements was about (0.76 ± 0.10) × 10⁻² cm/y. This value is in agreement with denudation rate reported by (Lauer and Willenbring, 2010), for Neuse river sediment samples (USA) (0.3 × 10⁻² cm/y). Lauer's denudation rate was calculated using equation (2) with the following considerations: steady state system, a negligible decay of the radionuclide, a deposition flux of meteoric ¹⁰Be of 12 × 10⁹ atom/m²/y. No data are present in the literature for the erosion rate using meteoric ¹⁰Be in surficial sediments except the ones reported by (Lauer and Willenbring, 2010). However, several studies can be found about the denudation rate assessment with ¹⁰Be “in situ”, measured in quartz (Table 3).

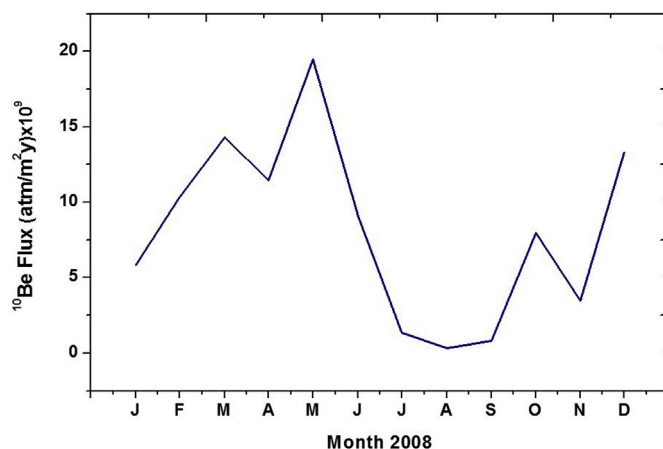


Fig. 6. Evolution of ¹⁰Be Flux on Guadiana River basin along 2008.

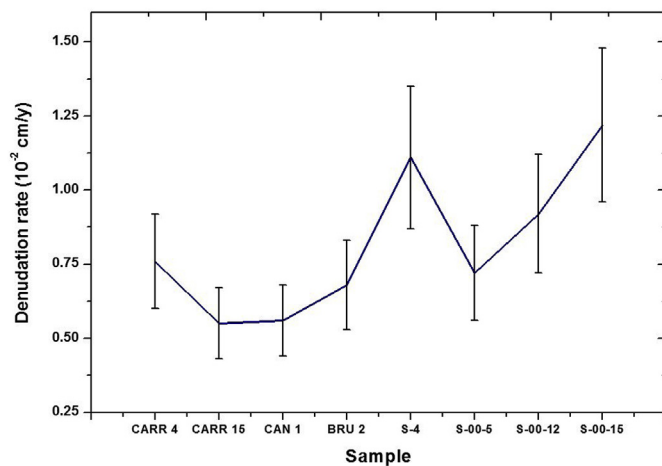


Fig. 7. Denudation rate (cm/y) for every sample using ^{10}Be concentration, the mean annual value of the total flux through the whole year of 2008 and density with equation (2).

6.2. Denudation rate by sediment budget method for the Guadiana river

The Guadiana estuarine is 60 km long, 550 m wide and its depth ranges from 5 to 17 m (Sampath et al., 2011). The mineralogical tests reported by (Morales González, 1995) showed that the sediment supplies detected in the estuarine come from four different sources: fluvial, coastal drift, marine environment and the direct supply from the superficial overflow of the estuarine itself.

The denudation rate estimated by the sediment budget method used the data reported by (Morales González, 1995) to obtain at least an estimation of the order of magnitude. After the calculation of the suspended sediment load (annual volume of sediment movement within the water column above the river bottom – 579 000 m^3/y) and bedload (annual volume of sediment movement over the river bottom – 439 600 m^3/y). Thus, the total output (O , equation (1)) sediment load into the sea from the river was $1.02 \times 10^6 \text{ m}^3/\text{y}$.

Based on morphological simulations using the HESM, the total volume deposited from 11500 to 7500 Cal y BP was about $3.05 \times 10^9 \text{ m}^3$ while the infilling volume of sediment since then was about $1.63 \times 10^9 \text{ m}^3$ to compensate for the increase of accommodation space due to sea-level rise during the Holocene period. A complete description of the numerical modelling approach to simulate the sediment infilling in the Guadiana Estuary since 11500 Cal y BP to present, is given in Sampath et al. (2015). Thus, the time weighted average of the fluvial sedimentation rate from 11500 Cal y BP to present due to sediment infilling (ΔS , equation (1)) was about $0.09 \times 10^6 \text{ m}^3/\text{y}$. Thus, the total fluvial sediment load (I , equation (1)) from the basin river was

estimated to be $1.11 \times 10^6 \text{ m}^3/\text{y}$ ($O + \Delta S = 0.09 \times 10^6 + 1.02 \times 10^6 \text{ m}^3/\text{y}$). The drainage area of the basin is $66\,960 \times 10^6 \text{ m}^2$. The denudation rate estimations by the sediment budget method according to (Morales González, 1995) was estimated as $1.66 \times 10^{-3} \text{ cm/y}$.

The uncertainty of the above estimation will depend on the estimation of sediment infilling rate of the estuary and total sediment transportation rates from the estuary. Large-scale geomorphological evolution of an estuarine system was simulated by means of a hybrid estuarine sedimentation model (HESM) applied to the Guadiana Estuary, in Southwest Iberia. The key controlling parameters of the model are bed friction (f), current velocity power of the erosion rate function (N), sea-level rise rate (Sampath and Boski, 2018) and estimations of river discharge (Sampath and Boski, 2016). The uncertainty of sediment infilling rate will mainly depend on the reconstruction of palaeovalley sea-level rise. However, the time taken to carry out the simulation of the sediment infilling in the Guadiana estuary from 11500 Cal y BP to present took was approximately about six months. This particle reason prevented the simulation of sediment infilling over the estuary by including the lower and upper limits of reconstructed palaeovalley sea-level rise curves. However, the average sea-level rise curve was used for the HESM simulations, which allowed a reasonable estimation of annual rate of sediment accumulation within the estuary.

The sedimentation rate used would be the most likely approximation for the maximum fluvial sedimentation rate over the Guadiana estuary assuming the estuary depth was kept pace with the sea-level rise over last 11500 Cal y BP and the marine sediment input was approximated to be 50% of total sediment deposited over the estuary during the Holocene. This approximation was based on the analysis of granulometric distribution of sediment types over the estuary and adjacent shore-face (Morales González, 1995).

The estimated value for the denudation rate is very comparable to the one reported by (Perez-Arлуca et al., 2005) for the Miñor river in northern Spain, which is 16 km long with a small reservoir in its course. Perez-Arлуca reported values around $1.01 \times 10^{-3} \text{ cm/y}$, from 2001 to 484 years BP and about $3.34 \times 10^{-3} \text{ cm/y}$ from 484 years BP to present date. These values are the same order of magnitude as the one obtained in this work.

However, the result obtained by the Sediment Budget method is much lower than the previously found from the ^{10}Be measurement. This disagreement is probably a result of the strong regulation that the Guadiana has suffered in the last 50 years. Because of this, the recent estimations of discharges of fluvial sediments cannot be representative of the anthropogenic periods. In 1990, about 70% of the Guadiana drainage basin was regulated and after the Alqueva Dam, river drainage regulation was increased to 81% and this resulted in a drastic reduction of sediment supply to estuary and oceanic basin (Domingues and Galvão, 2007; Morales González, 1995; Portela, 2006). At present, the water flow of the Guadiana river reaching the estuary is regulated by

Table 3

Comparison of the denudation/erosion rate obtained on several studies within ^{10}Be “in situ” with the obtained in this work with ^{10}Be “meteoric”.

Sediment Sample	Isotope	Denudation rate (10^{-2} cm/y)	Localisation	Reference
Beni River	^{10}Be “in situ”	4.55 ± 0.06	Andes, Bolivia	(Wittmann et al., 2009)
Mamore River	^{10}Be “in situ”	9.5 ± 4.4	Andes, Bolivia	(Wittmann et al., 2009)
Ecrins-Pelvoux massif	^{10}Be “in situ”	6.33 ± 0.76	Alps, France	(Delunel et al., 2010)
Eastern Altiplano Catchment	^{10}Be “in situ”	0.09 ± 0.01	Andes, Bolivia	(Hippe et al., 2012)
Napo River	^{10}Be “in situ”	3.14 ± 0.42	Andes, Peru-Ecuador	(Wittmann et al., 2011)
Lanyang River	^{10}Be “in situ”	18.8 ± 2.0	Taiwan, China	(Siame et al., 2011)
Ganga River	^{10}Be “in situ”	9.86 ± 0.89	Himalaya, India	(Lupker et al., 2012)
Rwenzori Mountain Sediments	^{10}Be “in situ”	0.60 ± 0.07	Uganda	(Roller et al., 2012)
Piura River Sediments	^{10}Be “in situ”	1.14 ± 0.15	Andes, Peru	(Abbühl et al., 2010)
Miño River Terrace	^{10}Be “in situ”	0.009 ± 0.001	Spain	(Viveen et al., 2012)
Betica Mountain Chain Sediments	^{10}Be “in situ”	0.63 ± 0.12	Spain	(Bellin et al., 2014)
Neuse River Sediments	^{10}Be “Meteoritic”	0.3	USA	(Lauer and Willenbring, 2010)
Guadiana River Sediments	^{10}Be “Meteoritic”	0.76 ± 0.10	Spain	This Work

more than 100 reservoirs, including the Alqueva reservoir, built in 2002. This has led to retain a big part of the sediment behind the dams compared to an unregulated river flow.

The ratio of the denudation rates obtained by the sediment budget method and the ^{10}Be method is 78.2%. This would approximately correspond to the amount, approximately 80%, of sediments that are retained behind the dams (Camacho et al., 2014; Dias and Ferreira, 2001; Rocha et al., 2002; Wolanski et al., 2006). If we assume that the sediment supplies into the ocean are also reduced by $80 \pm 5\%$, we may apply a correction for sediment accumulation behind dams along the Guadiana River. The above assumption is reasonable because the Guadiana estuary does not trap sediment within the basin at present but exports sediment into the sea. Thus, the almost all the sediment transported over the river discharge into the sea. There would be uncertainty in above estimation in short term (days to months) sediment infilling due to wave climate but the long-term (decadal to centennial scale) trend is a net sediment discharge into the sea. Therefore, the corrected denudation rate with one standard deviation of uncertainty around the average estimation using sediment budget method would be $(0.77 \pm 0.17) \times 10^{-2}$ cm/y.

Therefore, the denudation rate obtained by the sediment budget method with the appropriate corrections increased by one order of magnitude with respect to the value obtained previously. Hence, the above ratio obtained of 78.2% by both methods is reduced, reaching a value very much comparable with the one obtained by measuring of meteoric ^{10}Be in Guadiana river sediment samples, being $(0.76 \pm 0.10) \times 10^{-2}$ cm/y.

Though the uncertainties are high compared to a similar estimations that use annual flux averages, the order of magnitude of the denudation rate derived using the monthly flux average (in 2008) is compatible with the value obtained using sediment budget method. It is important to note that the calculations of the denudation rate using the sediment budget method are based on estimations of suspended load and bedload discharge from the Guadiana river by (Morales González, 1995). There are no published data on the sediment discharge of the Guadiana river; however, according to (Portela, 2006), the order of magnitude of both suspended load and bedload sediment discharge from 1980 to 2000 (before the Alqueva dam) were 10^5 m³/yr. In the context of rapid sea-level rise in the 21st century, the reduction of fluvial sediment supply due to the regulation of river discharge represents a major challenge for the management of estuarine ecosystems such as salt marshes. The reduction of sediment into the sea also result in severe erosion of the Guadiana coastal systems including its eastern shoreface. Therefore, it may be important to perform a study to estimate the total annual retention of sediment within dams and barrages along the Guadiana river.

7. Conclusions

The estimation of the denudation rate of the drainage in Lower Guadiana river catchment was done out using the concentration of meteoric ^{10}Be in sediment samples and confronted with the results obtained through the sediment budget method. The denudation rate of the Guadiana estuary derived from the ^{10}Be isotope method using annual average flux was $(0.76 \pm 0.10) \times 10^{-2}$ cm/y, while the denudation rate derived from the sediment budget method was 1.66×10^{-3} cm/y. The result derived by the measurement of radio-nuclide ^{10}Be is in line with the one reported by (Lauer and Willenbring, 2010) for Neuse river sediment samples (USA) and the one derived by sediment budget method is in total agreement with the one reported by (Perez-Arlucea et al., 2005) for Miñor river in northern of Spain. The difference between the values is attributed to the retention of large volume of fluvial sediments within the dam system along the Guadiana River, constructed during the last century. Therefore the value obtained by sediment budget method was corrected for a consensual $80 \pm 5\%$ attenuation of the sediment by the reservoirs. It yielded the rate of denudation $(0.77 \pm 0.17) \times 10^{-2}$ cm/y identical within the margin of

error to denudation rate obtained by ^{10}Be . Therefore, the ^{10}Be method is a very useful tool to carry out studies about processes of erosion within rivers. Despite their coherence these first results require further studies based on larger population of samples.

Acknowledge

This work has been financed through the projects FIS2012-31853 and FIS2015-69673-P provided by the Spanish Ministry of Economy and Competitiveness. We specially thank Ulla Heikkilä who provided us all data about the deposition flux of meteoric ^{10}Be by ECHAM5-HAM.

References

- Abbühl, L.M., Norton, K.P., Schlunegger, F., Kracht, O., Aldahan, A., Possnert, G., 2010. El Niño forcing on 10Be-based surface denudation rates in the northwestern Peruvian Andes? *Geomorphology* 123, 257–268. <https://doi.org/10.1016/J.GEOMORPH.2010.07.017>.
- Ahnert, F., 1970. Functional relationships between denudation, relief, and uplift in large, mid-latitude drainage basins. *Am. J. Sci.* 268, 243–263. <https://doi.org/10.2475/ajs.268.3.243>.
- Bellin, N., Vanacker, V., Kubik, P.W., 2014. Denudation rates and tectonic geomorphology of the Spanish Betic Cordillera. *Earth Planet Sci. Lett.* 390, 19–30. <https://doi.org/10.1016/J.EPSL.2013.12.045>.
- Boski, T., Moura, D., Veiga-Pires, C., Camacho, S., Duarte, D., Scott, D.B., Fernandes, S.G., 2002. Postglacial sea-level rise and sedimentary response in the Guadiana Estuary, Portugal/Spain border. *Sediment. Geol.* 150, 103–122. [https://doi.org/10.1016/S0037-0738\(01\)00270-6](https://doi.org/10.1016/S0037-0738(01)00270-6).
- Boski, T., Camacho, S., Moura, D., Fletcher, W., Wilamowski, A., Veiga-Pires, C., Correia, V., Loureiro, C., Santana, P., 2008. Chronology of the sedimentary processes during the postglacial sea level rise in two estuaries of the Algarve coast, Southern Portugal. *Estuar. Coast. Shelf Sci.* 77, 230–244. <https://doi.org/10.1016/J.ECSS.2007.09.012>.
- Calvo, E.C., Santos, F.J., López-Gutiérrez, J.M., Padilla, S., García-León, M., Heinemeier, J., Schnabel, C., Scognamiglio, G., 2015. Status report of the 1 MV AMS facility at the Centro Nacional de Aceleradores. *Nucl. Instrum. Methods Phys. Res. Sect. B Beam Interact. Mater. Atoms* 361, 13–19. <https://doi.org/10.1016/J.NIMB.2015.02.022>.
- Camacho, S., Moura, D., Connor, S., Boski, T., Gomes, A., 2014. Geochemical characteristics of sediments along the margins of an atlantic-mediterranean estuary (the Guadiana, Southeast Portugal): spatial and seasonal variations. *Rev. Gestão Costeira Integr.* 14, 129–148. <https://doi.org/10.5894/rgci452>.
- Delgado, J., Barba-Brioso, C., Nieto, J.M., Boski, T., 2011. Speciation and ecological risk of toxic elements in estuarine sediments affected by multiple anthropogenic contributions (Guadiana saltmarshes, SW Iberian Peninsula): I. Surficial sediments. *Sci. Total Environ.* 409, 3666–3679. <https://doi.org/10.1016/J.SCITOTENV.2011.06.013>.
- Delgado, J., Boski, T., Nieto, J.M., Pereira, L., Moura, D., Gomes, A., Sousa, C., García-Tenorio, R., 2012. Sea-level rise and anthropogenic activities recorded in the late Pleistocene/Holocene sedimentary infill of the Guadiana Estuary (SW Iberia). *Quat. Sci. Rev.* 33, 121–141. <https://doi.org/10.1016/J.QUASCIREV.2011.12.002>.
- Delunel, R., van der Beek, P.A., Carcaillet, J., Bourlès, D.L., Valla, P.G., 2010. Frost-cracking control on catchment denudation rates: insights from in situ produced 10Be concentrations in stream sediments (Ecrins–Pelvoux massif, French Western Alps). *Earth Planet Sci. Lett.* 293, 72–83. <https://doi.org/10.1016/J.EPSL.2010.02.020>.
- Dias, J.A., Ferreira, Ó., 2001. Projecto EMERGE – Estudo Multidisciplinar Do Estuário Do Rio Guadiana. Relatório Final 3/01. CIACOMAR. Universidade do Algarve, Olhão, Portugal. http://w3.uaalg.pt/~jdias/JAD/ebooks/EMERGE/EMERGE_total_red.pdf.
- Domingues, R.B., Galvão, H., 2007. Phytoplankton and environmental variability in a dam regulated temperate estuary. *Hydrobiologia* 586, 117–134. <https://doi.org/10.1007/s10750-006-0567-4>.
- Ebert, K., Willenbring, J., Norton, K.P., Hall, A., Hättestrand, C., 2012. Meteoric 10Be concentrations from saprolite and till in northern Sweden: implications for glacial erosion and age. *Quat. Geochronol.* 12, 11–22. <https://doi.org/10.1016/j.quageo.2012.05.005>.
- Field, C., Schmidt, G.A., Koch, D., 2005. Solar and climatic effects on Beryllium-10. *In: Mem. S.A.It.*, 76: 805.
- Field, C.V., Schmidt, G.A., Koch, D., Salyk, C., 2006. Modeling production and climate-related impacts on ^{10}Be concentration in ice cores. *J. Geophys. Res.* 111 D15107. <https://doi.org/10.1029/2005JD006410>.
- Fortunato, A.B., Oliveira, A., 2004. A modeling system for tidally driven long-term morphodynamics. *J. Hydraul. Res.* 42, 426–434. <https://doi.org/10.1080/00221686.2004.9728408>.
- Galvão, H., Reis, M., Dominguez, R., Caetano, S., Mesquita, S., Barbosa, A., Costa, C., Vilchez, C., Teixeira, M., 2012. Ecological tools for the management of cyanobacteria blooms in the Guadiana river watershed, southwest iberia. *In: Studies on Water Management Issues. InTech.* <https://doi.org/10.5772/28283>.
- Garel, E., Pinto, L., Santos, A., Ferreira, Ó., 2009. Tidal and river discharge forcing upon water and sediment circulation at a rock-bound estuary (Guadiana estuary, Portugal). *Estuar. Coast Shelf Sci.* 84, 269–281. <https://doi.org/10.1016/j.eccs.2009.07.002>.
- Graly, J.A., Bierman, P.R., Reusser, L.J., Pavich, M.J., 2010. Meteoric ^{10}Be in soil profiles - a global meta-analysis. *Geochim. Cosmochim. Acta* 74, 6814–6829. <https://doi.org/10.1016/j.gca.2010.08.036>.

- Gregory, K.J., Goudie, A., 2011. *The SAGE Handbook of Geomorphology*. SAGE.
- Gutjahr, M., Frank, M., Stirling, C.H., Klemm, V., van de Fliedert, T., Halliday, A.N., 2007. Reliable extraction of a deepwater trace metal isotope signal from Fe–Mn oxyhydroxide coatings of marine sediments. *Chem. Geol.* 242, 351–370. <https://doi.org/10.1016/J.CHEMGEO.2007.03.021>.
- Heikkilä, U., 2007. Modeling of the Atmospheric Transport of the Cosmogenic Radionuclides 10Be and 7Be Using the ECHAM5-ham General Circulation Model.
- Heikkilä, U., Smith, A.M., 2013. Production rate and climate influences on the variability of ¹⁰Be deposition simulated by ECHAM5-HAM: globally, in Greenland, and in Antarctica. *J. Geophys. Res. Atmos.* 118, 2506–2520. <https://doi.org/10.1002/jgrd.50217>.
- Heikkilä, U., Beer, J., Feichter, J., 2009. Meridional transport and deposition of atmospheric ¹⁰Be. *Atmos. Chem. Phys.* 9, 515–527. <https://doi.org/10.5194/acp-9-515-2009>.
- Hippe, K., Kober, F., Zeilinger, G., Ivy-Ochs, S., Maden, C., Wacker, L., Kubik, P.W., Wieler, R., 2012. Quantifying denudation rates and sediment storage on the eastern Altiplano, Bolivia, using cosmogenic ¹⁰Be, ²⁶Al, and in situ ¹⁴C. *Geomorphology* 179, 58–70. <https://doi.org/10.1016/J.GEOMORPH.2012.07.031>.
- Klein, M.G., Mous, D.J.W., Gottang, A., 2006. A compact 1 MV multi-element AMS system. *Nucl. Instrum. Methods Phys. Res. Sect. B Beam Interact. Mater. Atoms* 249, 764–767. <https://doi.org/10.1016/J.NIMB.2006.03.135>.
- Lachner, J., Christl, M., Sinal, H.-A., Frank, M., Jakobsson, M., 2013. Carrier free ¹⁰Be/⁹Be measurements with low-energy AMS: determination of sedimentation rates in the Arctic Ocean. *Nucl. Instrum. Methods Phys. Res. Sect. B Beam Interact. Mater. Atoms* 294, 67–71. <https://doi.org/10.1016/J.NIMB.2012.07.016>.
- Lauer, J.W., Willenbring, J., 2010. Steady state reach-scale theory for radioactive tracer concentration in a simple channel/floodplain system. *J. Geophys. Res.* 115 F04018. <https://doi.org/10.1029/2009JF001480>.
- Lupker, M., Blard, P.-H., Lavé, J., France-Lanord, C., Leanni, L., Puchol, N., Charreau, J., Bourlès, D., 2012. ¹⁰Be-derived Himalayan denudation rates and sediment budgets in the Ganga basin. *Earth Planet Sci. Lett.* 333–334, 146–156. <https://doi.org/10.1016/J.EPSL.2012.04.020>.
- Martínez-Aldaya, M., Llamas, M.R., 2009. *Water Footprint Analysis (Hydrologic and Economic) of the Guadiana River Basin*.
- Masarik, J., Beer, J., 1999. Simulation of particle fluxes and cosmogenic nuclide production in the Earth's atmosphere. *J. Geophys. Res. Atmos.* 104, 12099–12111. <https://doi.org/10.1029/1998JD200091>.
- Morales González, J.A., 1995. *Sedimentología del estuario del Río Guadiana*. Industrias Químicas y Básicas, S.O. España-Portugal.
- Nishiizumi, K., Imamura, M., Caffee, M.W., Southon, J.R., Finkel, R.C., McAninch, J., 2007. Absolute calibration of ¹⁰Be AMS standards. *Nucl. Instrum. Methods Phys. Res. Sect. B Beam Interact. Mater. Atoms* 258, 403–413. <https://doi.org/10.1016/J.NIMB.2007.01.297>.
- Padilla Domínguez, S., 2015. *Medidas de ¹⁰Be y ²⁶Al en espectrometría de masas con acelerador de baja energía en el Centro Nacional de Aceleradores*.
- Perez-Arlucea, M., Mendez, G., Clemente, F., Nombela, M., Rubio, B., Filgueira, M., 2005. Hydrology, sediment yield, erosion and sedimentation rates in the estuarine environment of the Ria de Vigo, Galicia, Spain. *J. Mar. Syst.* 54, 209–226. <https://doi.org/10.1016/J.JMARSYS.2004.07.013>.
- Portela, L.L., 2006. Calculation of sediment delivery from the Guadiana estuary to the coastal. *J. Coast Res.* <https://doi.org/10.2307/25743075>.
- Reid, Leslie M., Dunne, Thomas, 2000. Rapid evaluation of sediment budgets. In: *Earth Surf. Process. Landforms*, vol 25. Catena Verlag, Reiskirchen, 3-923381-39-5, pp. 1275. [https://doi.org/10.1002/1096-9837\(200010\)25:11<1275::AID-ESP152>3.0.CO;2-Y](https://doi.org/10.1002/1096-9837(200010)25:11<1275::AID-ESP152>3.0.CO;2-Y).
- Reid, L.M., Dunne, T., Cederholm, C.J., 1981. Application of Sediment Budget studies to the evaluation of logging road impact. *J. Hydrol. (New Zealand)*. <https://doi.org/10.2307/43945095>.
- Rocha, C., Galvão, H., Barbosa, A., 2002. Role of transient silicon limitation in the development of cyanobacteria blooms in the Guadiana estuary, south-western Iberia. *Mar. Ecol. Prog. Ser.* 228, 35–45. <https://doi.org/10.3354/meps228035>.
- Roller, S., Wittmann, H., Kastowski, M., Hinderer, M., 2012. Erosion of the rwenzori mountains, east african rift, from in situ-produced cosmogenic ¹⁰Be. *J. Geophys. Res. Earth Surf.* 117 n/a-n/a. <https://doi.org/10.1029/2011JF002117>.
- Sampath, D.M.R., Boski, T., 2016. Morphological response of the saltmarsh habitats of the Guadiana estuary due to flow regulation and sea-level rise. *Estuar. Coast Shelf Sci.* 183, 314–326. <https://doi.org/10.1016/j.ecss.2016.07.009>.
- Sampath, D.M.R., Boski, T., 2018. Key parameters of the sediment surface morphodynamics in an estuary – an assessment of model solutions. *Geomorphology* 308, 142–160. <https://doi.org/10.1016/J.GEOMORPH.2018.02.017>.
- Sampath, D.M.R., Boski, T., Silva, P.L., Martins, F.A., 2011. Morphological evolution of the Guadiana estuary and intertidal zone in response to projected sea-level rise and sediment supply scenarios. *J. Quat. Sci.* 26, 156–170. <https://doi.org/10.1002/jqs.1434>.
- Sampath, D.M.R., Boski, T., Loureiro, C., Sousa, C., 2015. Modelling of estuarine response to sea-level rise during the Holocene: application to the Guadiana estuary–SW Iberia. *Geomorphology* 232, 47–64. <https://doi.org/10.1016/J.GEOMORPH.2014.12.037>.
- Siame, L.L., Angelier, J., Chen, R.-F., Godard, V., Derriex, F., Bourlès, D.L., Braucher, R., Chang, K.-J., Chu, H.-T., Lee, J.-C., 2011. Erosion rates in an active orogen (NE-Taiwan): a confrontation of cosmogenic measurements with river suspended loads. *Quat. Geochronol.* 6, 246–260. <https://doi.org/10.1016/J.QUAGEO.2010.11.003>.
- Slaymaker, O., 2003. The sediment budget as conceptual framework and management tool. *Hydrobiologia* 494, 71–82. <https://doi.org/10.1023/A:1025437509525>.
- Viveen, W., Braucher, R., Bourlès, D., Schoorl, J.M., Veldkamp, A., van Balen, R.T., Wallinga, J., Fernandez-Mosquera, D., Vidal-Romani, J.R., Sanjurjo-Sanchez, J., 2012. A 0.65 Ma chronology and incision rate assessment of the NW Iberian Miño River terraces based on ¹⁰Be and luminescence dating. *Glob. Planet. Change* 94–95, 82–100. <https://doi.org/10.1016/J.GLOPLACHA.2012.07.001>.
- von Blanckenburg, F., 2005. The control mechanisms of erosion and weathering at basin scale from cosmogenic nuclides in river sediment. *Earth Planet Sci. Lett.* 237, 462–479. <https://doi.org/10.1016/J.EPSL.2005.06.030>.
- von Blanckenburg, F., Belshaw, N.S., O'Nions, R.K., 1996. Separation of ⁹Be and cosmogenic ¹⁰Be from environmental materials and SIMS isotope dilution analysis. *Chem. Geol.* 129, 93–99. [https://doi.org/10.1016/0009-2541\(95\)00157-3](https://doi.org/10.1016/0009-2541(95)00157-3).
- von Blanckenburg, F., Bouchez, J., Wittmann, H., 2012. Earth surface erosion and weathering from the ¹⁰Be (meteoric)/⁹Be ratio. *Earth Planet Sci. Lett.* 351–352, 295–305. <https://doi.org/10.1016/J.EPSL.2012.07.022>.
- Wasson, R.J., 2003. A sediment budget for the Ganga–Brahmaputra catchment. *Curr. Sci.* <https://doi.org/10.2307/24107666>.
- Willenbring, J.K., von Blanckenburg, F., 2010. Meteoric cosmogenic Beryllium-10 adsorbed to river sediment and soil: applications for Earth-surface dynamics. *Earth Sci. Rev.* 98, 105–122. <https://doi.org/10.1016/j.earscirev.2009.10.008>.
- Wittmann, H., von Blanckenburg, F., Guyot, J.L., Maurice, L., Kubik, P.W., 2009. From source to sink: preserving the cosmogenic ¹⁰Be-derived denudation rate signal of the Bolivian Andes in sediment of the Beni and Mamoré foreland basins. *Earth Planet Sci. Lett.* 288, 463–474. <https://doi.org/10.1016/J.EPSL.2009.10.008>.
- Wittmann, H., von Blanckenburg, F., Guyot, J.L., Laraque, A., Bernal, C., Kubik, P.W., 2011. Sediment production and transport from in situ-produced cosmogenic ¹⁰Be and river loads in the Napo River basin, an upper Amazon tributary of Ecuador and Peru. *J. South Am. Earth Sci.* 31, 45–53. <https://doi.org/10.1016/J.JSAMES.2010.09.004>.
- Wolanski, E., Chicharo, L., Chicharo, M.A., Morais, P., 2006. An ecohydrology model of the Guadiana estuary (south Portugal). *Estuar. Coast Shelf Sci.* 70, 132–143. <https://doi.org/10.1016/J.ECSS.2006.05.029>.